Chapter – 1
Introduction

1.1. Brief history of materials design

Growing environmental concerns, continuous depletion of fossil fuel reserves and changing geo-political scenario has incentivized the search for new energy resources and technologies [1-5]. It has been well understood that future sustainable and green energy revolutions will be driven by the innovations of materials [4-7]. Modern day civilization relies heavily on the production and processing of numerous materials at very large scales for a plethora of applications. This includes bulk production of innumerable kinds of materials for manufacturing familiar daily life objects to components for critical engineering applications [8,9]. India alone produces over 100 MT of crude steel every year for its use in construction, automobile and allied industries, whereas Taiwan on its own produces more than 15 million semiconductor wafer microchips per year for application in the fields of physical and biological sciences, sports and entertainment alike [10,11]. Interestingly, our ancestors from prehistoric times too depended on various materials, however on a much more modest scale. Weapons, tools, ornaments and artworks were forged from simple materials which would help in protecting themselves (survival of the fittest) while at the same time hunt effectively and migrate efficiently. A schematic representing the chronological evolution of materials along with the human race is presented in Figure 1.1. Since time immemorial, stone and wood were extensively used to perform miraculous things of the time, lighting fire and making wheels. After a few thousand centuries of stone age and crudities of our neolithic ancestors, the chalcolithic period saw man using native metals like copper, tin, lead and arsenic for the first time [12]. In this era of early metallurgists, people quickly realized how to extract metals from their relatively pure naturally occurring mineral ores and once extracted they could be hardened by repeated hammering (forging). Gold and silver also caught attention due to their luster but were too soft to be used in anything apart from ornamentation and craft. However, the

importance of gold as a precious metal led to the dishonest mixing of other elements in small quantities and thus the art of alloying was brewed for the first time. This led to the explosion from copper age to bronze age. People soon realized that alloying makes a material stronger and easier to cast into various shapes than their monolithic counterparts. Alloying, which started as an accidental malpractice ~5000 years ago, soon became a quintessential practice and continues to thrive to this day [13]. The historical milestone of the industrial revolution and renaissance in many parts of the world may directly be attributed to the age-old cumulative understanding of metallurgy and materials, which then started to bloom as a young subject of science [14]. It is now one of the most fascinating interdisciplinary branches of science today. Thus, metallurgy and materials knowledge evolved from rudimentary art to state-of-the-art science over thousands of years, with incremental progress until recently. Current advances in science and technology have brought us at the forefronts of materials exploration [4-9].

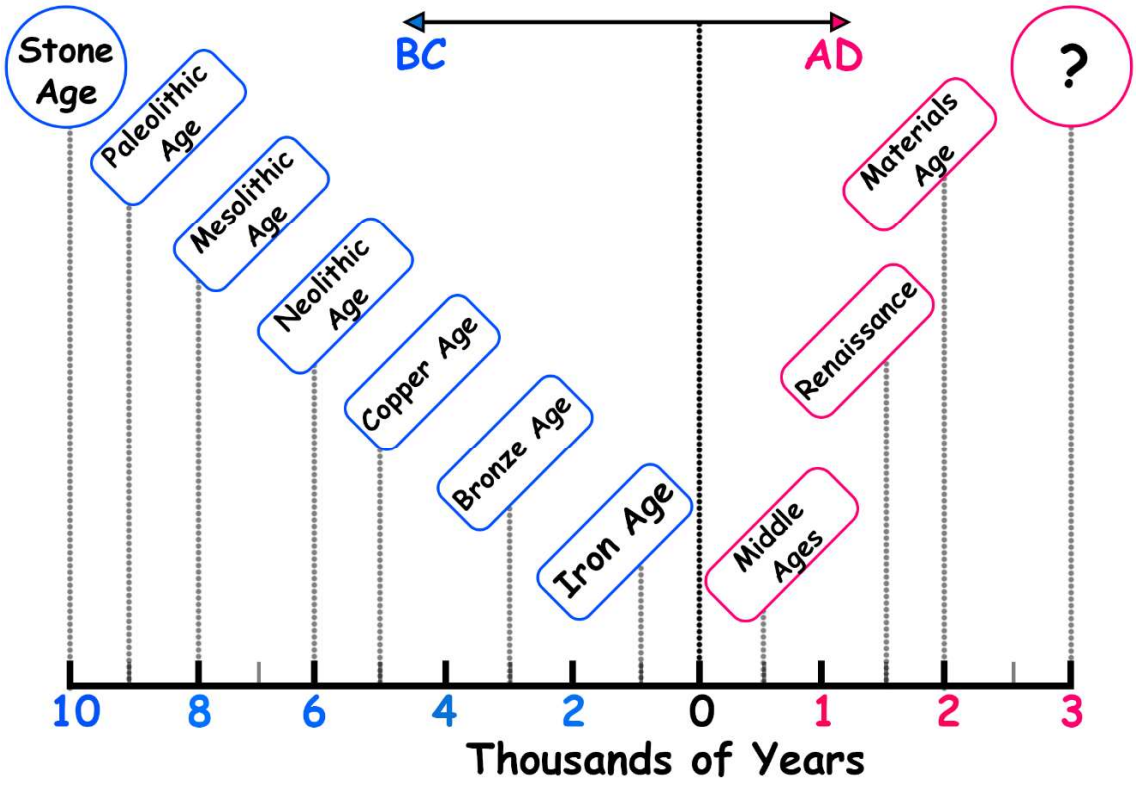

Figure 1.1: Schematic representing the long arduous journey of pre-historic humans in relationship with materials, which in turn holds huge promise for the future.

Materials design encompasses a broad knowledge-based approach in discovering and/or synthesizing materials with a desired combination of properties. Traditionally, there was no well laid principle to arrive at a particular composition with a specific structure and specific set of properties. Empiricism-based heuristic approach has led traditional metallurgists to design alloys/materials for various applications. This approach demands observing a large number of material systems so as to decipher underlying patterns and it heavily relies on the researcher's experience, grasp over the subject, intuition-driven trial-and-error and serendipity [15,16]. Hume-Rothery rules for solid-solution formation, Inoue's criteria for glass formation, Pettifor structure maps for synthesis of intermetallic compounds and Pauling's rules for formation of ionic materials are some of the notable achievements of the age-old heuristic approach [17-20]. However, this approach is not being able to keep pace with the modern-day scenario where there is an ever-increasing demand for materials. In the field of engineering alone, more than 1000 different types of metallic alloys are being used daily [21]. Regardless, this is a miniscule fraction of the possible number of alloys that can be synthesized [22]. In this context, inverse-heuristic approach is gaining momentum with the advent of data mining and machine learning. The new-age materials design adopts a forward or "function follows form" approach. It involves several descriptors namely atomic identity, chemistry and structure (ACS) as input parameters to ensue specific material output properties. However, with the advancement in computational prowess, a contrary approach where the desired target properties are used as an input to determine the ACS which in turn can reveal the material composition space, is being explored. This is the "form follows function" inverse-heuristic design philosophy [23,24]. In the author's opinion, old-fashioned heuristic approach is irreplaceable, although clubbed with data mining, modelling and simulation is bound to make newer materials exploration more exciting. A brief review of materials design philosophy over the last

century and a paradigm shift in it are presented in this chapter. The chapter culminates with identifying the scientific bottlenecks in the field thus far and formulate problem statements which shall serve as the objectives of the thesis.

1.2. Metallic alloys and compounds

1.2.1. Traditional multicomponent alloys

The early 19th century witnessed the birth of inductive reasoning and observation-based empiricism and its father is widely regarded as Francis Bacon. Soon, most of the demand for robust alloys were propelled by core manufacturing industries of automobile, electrical and construction sectors [14]. Development of grain-oriented texture in Fe-Si alloy, along with other minor alloying elements, by controlled heat-treatment schedule for transformer core laminations was one of the first concise alloy design strategies to be adopted successfully at industrial scales [25]. In this context, seminal works of Sorby (birth of metallography), Matthiessen (conductivity in alloys), Bozorth (Invar), Barrett (silicon-iron), Seebeck (thermoelectricity), Graham and Sieverts (gas occlusions in metals), Zackay (TRIP steel), Bauschinger (deformation of metals), Buerger (deformation micromechanics) are worth mentioning [15]. The discovery of x-rays by Roentgen during beginning of the 20th century followed by the invention of Transmission Electron Microscope by Ruska and Knolls shortly after, completely transformed the dimensions of the subject [26,27]. This led eminent scientists such as Bragg and Bragg, Von Laue, Ewald, Otto Müller and others to directly investigate the microstructure at unprecedented resolution and indirectly explore the crystal structure of crystalline materials [28,29]. On top of that, seminal works on equilibrium constitutional diagrams for binary alloys during this period made alloy design a very conscious strategy for several varied applications [30]. In this regard, the traditional alloys were mainly composed of one element (in principal amount) alloyed with several

elements in non-major proportions. They were commonly referred to as “dilute alloys” or X-based alloys (X: element in principal amount). A list of note-worthy dilute alloys is mentioned in Figure 1.2. along with their rough timeline of development.

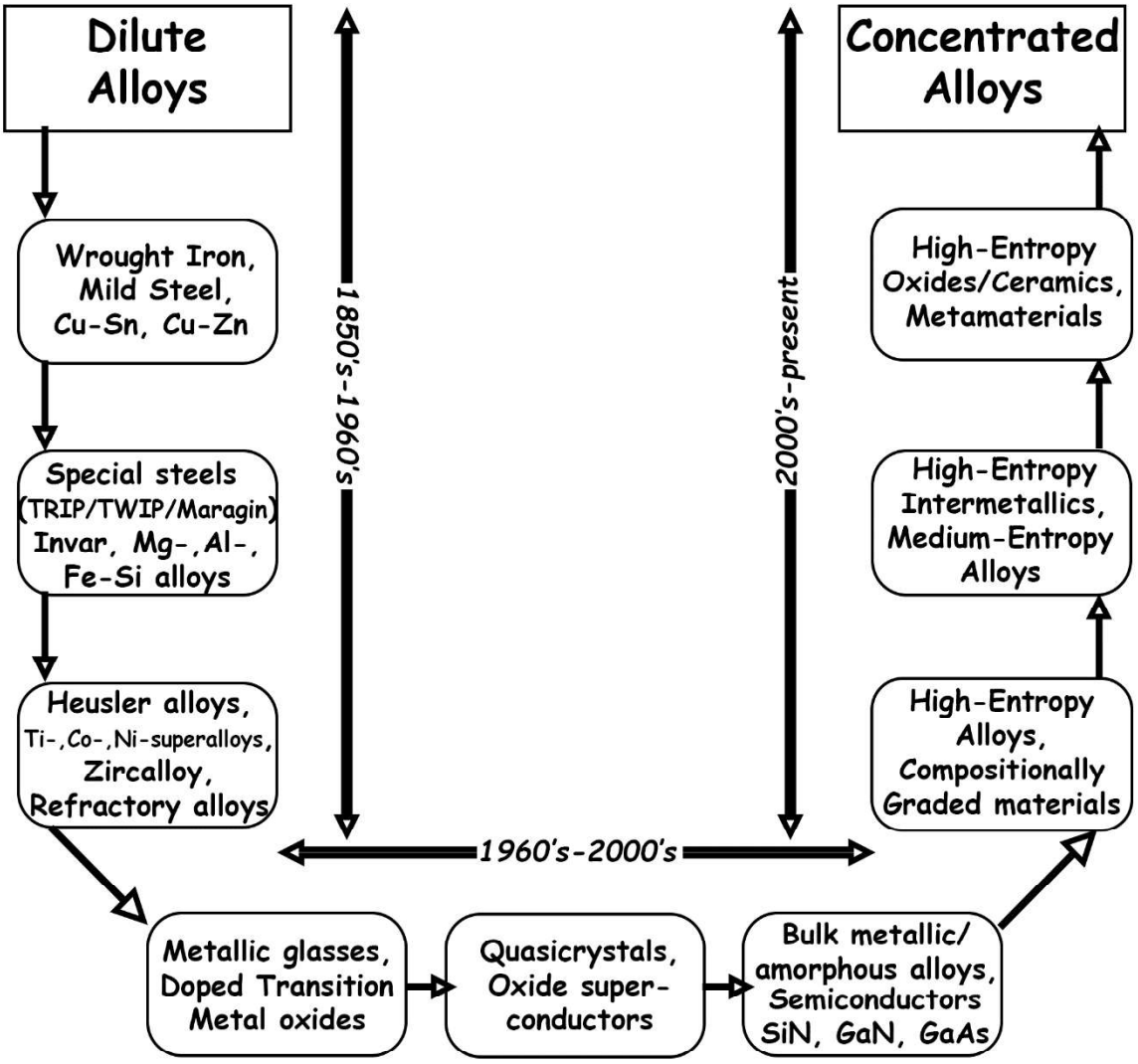

Figure 1.2: Broad categorization of profound engineering materials based on their alloy design strategy and their estimated timeline of evolution during the last two centuries.

The most notable dilute alloy is steel with 40-85 wt% Fe, 0.08-2 wt% C and balance other alloying elements, which in itself is a broad subject of study owing to its versatility, diversity and relevancy even to this day [31-33]. A typical microstructure of steel usually consists of multiple phases predicted by Gibbs phase rule from Fe-$C_{equivalent}$ constitution

diagram (in case of near equilibrium processing) or from TTT/CCT diagrams (for non-equilibrium processing). It then becomes possible to engineer the second phase(s) in terms of shape, size, distribution, volume fraction to achieve strength-ductility tradeoff, a common performance barrier well-documented in steel literature [34]. Expanding to non-ferrous alloys, it was systematically reported that several multi-phase dilute alloys often yield good combination of properties while many do not. The Ni-based superalloy may be cited as one such example where the γ/γ' dual-phase microstructure with shape-controlled ordered domains within the matrix phase provides excellent properties even at elevated temperatures [35,36]. Additionally, Ti-6Al-4V is an ($\alpha+\beta$)-Ti alloy and is commonly regarded as Ti-superalloy [37]. On the other hand however, most β-Ti alloys suffer from poor combination of properties due to ω-phase transformation products [38,39]. It is because of the heavy mismatch of active slip systems in the BCC matrix of β-Ti when compared to hexagonal (complete-collapse) or trigonal (partially-collapse) ω nano-domains, that crack generation and propagation gets favoured along the interphase interfaces, causing embrittlement and premature failure of structural components [40,41]. A quintessential strategy in alloy development, after a general composition is ball-parked, is to seek explanations to fundamental root causes of failure or poor performance and how to favourably engineer them. This helps to develop better structure-property-performance co-relationships and strategies to make existing alloys better. Hence tremendous efforts have been put over several decades in the areas of material processing and heat-treatment induced strengthening mechanisms so as to improve the performance of the existing dilute alloys [31-41].

During this period, Hume-Rothery postulated few empirical rules for extensive solid-solubility considering the atomic size, electronegativity and crystal structure of individual elements, which is useful to this day [42]. These rules could predict, barring a few

exceptions, simple isomorphous (complete miscibility across entire composition range) systems from that of limited solubility systems coupled with one or more invariant reactions. This qualitative approach in tandem with thermodynamic descriptors and advanced metallographic techniques of the time proved to be a great combination in designing and processing newer alloys of both ferrous and non-ferrous nature with huge success [43,44].

1.2.2. Bulk metallic glasses

Turnbull and Duwez demonstrated for the first time a rapid solidification technique which was able to produce cooling rates as high as 10^6 K/second in their seminal work during late 1950's [45,46]. The first liquid alloy to be vitrified by cooling from the molten state was Au-Si alloy [47]. Decades after this discovery, dozens of ferrous and non-ferrous alloy systems were found to form glasses over a wide range of composition [46]. There is usually no recalescence process associated with glass formation and thus it is categorized as a 2^{nd}-order phase transformation under Landau scheme of phase transitions. The characteristic microstructural feature is the amorphous structure of the alloy with electron diffraction revealing diffuse-ring pattern [48-50]. Amorphization of an alloy essentially involves the kinetic suppression of nucleation and growth from its undercooled melt. Initially, the glassy state was understood from Kauzmann's paradox of undercooling [51]. It depicts a scenario where the entropy of molten liquid (above the melting point) when extrapolated backwards under the action of undercooling, becomes lower than the entropy of the solid phase of the same composition, which is absurd. To avoid this absurdity, the system chooses to be in a glassy-state without crystallizing. However, such high cooling rates posed a practical difficulty in the dimensions of the rapidly cooled alloy, often restricting specimen geometry to thin foils, ribbons or powder [47]. Metallurgists of the time started dreaming of newer alloys that could form glasses at much lower cooling rates like their silicate glass

counterpart, which would realize their production in bulk form as well as in bulk quantities. After almost thirty years of research in the field of metallic glasses, pioneering work by Inoue during late 1980's and Johnson a decade later, catapulted the emerging field to new heights and bulk metallic glasses (BMG's) were born [52,53]. A number of La-, Mg-, Zr-, Ti-, Pd-, Fe-, Al-, and Ni-bearing glass formers were identified which could be vitrified with cooling rates as low as 0.1 K/second [53-55]. They could also be cast into 12mm diameter rods [55]. This development directly extended the opportunity to understand long-standing problems in solidification science and the structure of the liquid phase of the alloys. Extensive research in BMG's often captured precipitation of nano crystals/quasicrystals upon cooling, establishing a link with possible short-range order (SRO) in the liquid state, which is proven to be a statement of fact with advancement of electron microscopy [56-59].

Several empirical criteria for formation of BMG's were proposed by Inoue which later became synonymous with inverse Hume-Rothery criteria for solid-solution formation [49]. Inoue argued that multicomponent alloys with large atomic radii mismatch between constituent elements and highly negative heats of mixing between each pair of binaries should favour glass formation [52]. This is why constitution diagrams with deep eutectics and intermetallics are prone to glass formation [53-55]. It is envisaged that geometric frustration in the lattice, if allowed to exceed beyond a certain threshold can structurally destabilize the lattice from crystallizing and hence solidify in a glassy-state.

1.2.3. Multiprincipal elemental alloys

High entropy alloys (HEAs) were brought into existence by innovative thinking coupled with a dash of serendipity by Cantor and Yeh, independently during 2004-05 [60,61]. They argued in favour of little or no data on ternary, quaternary, quinary and subsequent higher-

order constitution diagrams which has confined traditional metallurgists to explore alloys based on one or two components in principal amounts only. Although this approach has enriched the database of alloys pertaining to the corners/edges of the binary and to some extent ternary constitution diagrams, it also has led to the center composition-space of higher-order equilibrium diagrams practically unexplored [60].

In binary or ternary dilute alloys, physical metallurgists are primarily concerned about solid-solution phases and invariant reaction products at the terminal ends of the diagram. This is usually because of the formation of hard and brittle topologically packed intermetallic and vacancy-ordered phase(s) at the centers of the phase diagram, most prominent example being the Al-Ni phase diagram [62,63]. Linearly extrapolating the argument to the center composition-space of higher order systems, predict several secondary phases in accordance to the Gibbs phase rule. However, it is counterintuitive to find one or two simple solid-solution phase(s) when a large number of elements (≥5) are mixed in principal (equiatomic or near-equiatomic) amounts [61]. This has been coined as the "High Entropy" effect which constitutes one of the four core effects in concentrated alloys, apart from "sluggish diffusion", "lattice distortion" and "cocktail effect" which are well documented in literature [64-67]. The birth of such concentrated alloys of 5-6 or more elements in equiatomic or near equiatomic ratio exponentially increased the number of alloys that could be formed and studied, which was previously unanticipated. A simple palette of 40 elements from the periodic table if alloyed in equiatomic or near equiatomic proportions offers a possibility of ~10^{10} multiprincipal elemental alloys [22]. An explosion of materials research based on the newly formulated alloy design technique yielded several novel classes of materials which is summarized in Figure 1.3 [68-71].

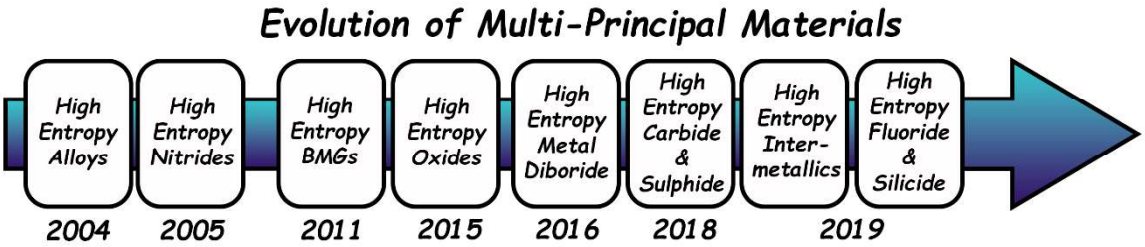

Figure 1.3: Fruits of concentrated alloy design strategy.

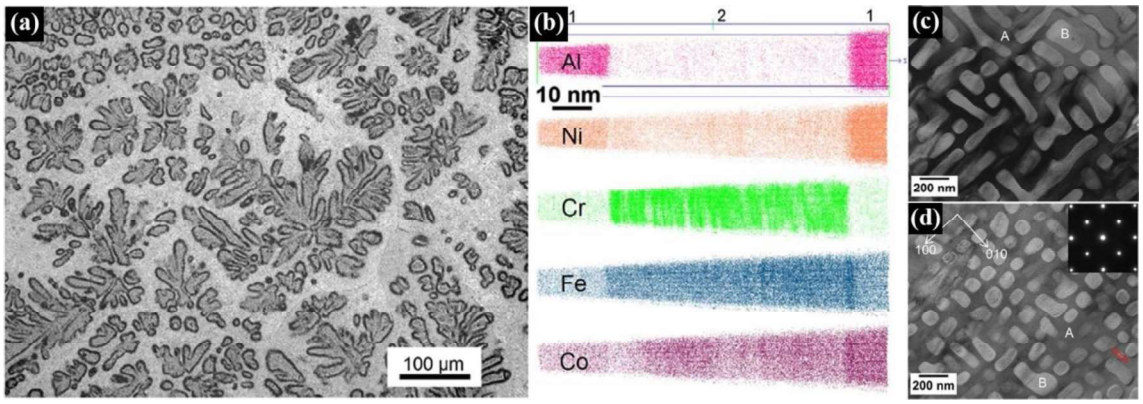

Figure 1.4: As-cast AlCoCrFeNi HEA (a) optical micrograph showing dendritic solidification, (b) 3D reconstruction of Al, Co, Cr, Fe and Ni atoms from APT experiment and (c,d) TEM BF images of dendritic and interdendritic phase with definite morphology. The dark contrast matrix phase (marked as A) is Al-Ni rich while the bright precipitate phase (marked as B) is Cr-Fe rich [77].

The high entropy effect has been attributed to the overwhelming dominance of configurational entropy of mixing (ΔS_{mix}), which would always offset enthalpy of mixing (ΔH_{mix}) term in the free energy equation and consequently in the energy landscape of the alloy [72]. Hence, it was believed that such a thermodynamic mandate holds the clue to simple solid-solution phase formation, with randomly distributed motifs in the disordered lattice. However, it was a matter of time before the scientific community found out through careful experimentation that almost all the HEAs were not phase pure [73,74]. Even if in rare instances some of them like CoCrFeMnNi Cantor alloy were established to be single-phase, it was later found to be metastable with respect to time-temperature assisted phase separation events [75,76]. Thus, what started out as clean microstructures composed of

simple solid-solution phase, turned out to be highly complex in due course of research. One such example of microstructural evolution from AlCoCrFeNi HEA processed via solid-state route and consolidated by spark plasma sintering is shown in Figure 1.4 [77]. It depicts a two-phase mixture of sub-micron sized ordered BCC second phase decorating a disordered BCC matrix phase. Furthermore, transmission electron microscopy in conjunction with spectroscopy has revealed nanoprecipitates, ordered solid-solution phases, intermetallic phases, amorphous phases and short-range order domains in numerous alloys. These observations essentially hint at the shortcomings of the oversimplified model for entropic stabilization in multiprincipal elemental alloys [22, 73-77].

1.3. High entropy oxides

This class of materials were conceived following the lines of high entropy alloys by Maria and Rost in 2015 [78]. The model high entropy oxide (HEO) system is the equimolar mixture of Co^{+2}, Cu^{+2}, Mg^{+2}, Ni^{+2} and Zn^{+2} which forms a phase-pure solid-solution phase with the cubic rocksalt (MO) structure. Their work demonstrated entropic reversibility i.e. transformation of multi-phase to single-phase above a threshold sintering temperature and back to multi-phase on lowering the temperature [78,79]. This was achieved by in-situ heating XRD experiment. STEM-EDS too revealed random distribution of cations in the ordered oxygen sub-lattice ion columns. These observations convinced the scientific community to promote this particular composition of HEO as entropy stabilized oxide (ESO) with homogeneous single-phase structure, which is a subset of HEO and in turn of multiprincipal materials. This has been depicted in Figure 1.5. With the discovery of high entropy oxide, a host of several classes of high entropy oxides based on different crystal structures evolved. A comprehensive list is shown in Figure 1.6, which is far from exhaustive since novel oxides are continuously being synthesized [80-82].

Although the material design premise of HEOs is an extension to the principles of HEAs, there are certain fundamental distinctions between the two. A HEO has two separate sublattices for cation and anion compared to a single lattice framework for HEA [78]. However, that is just one scenario.

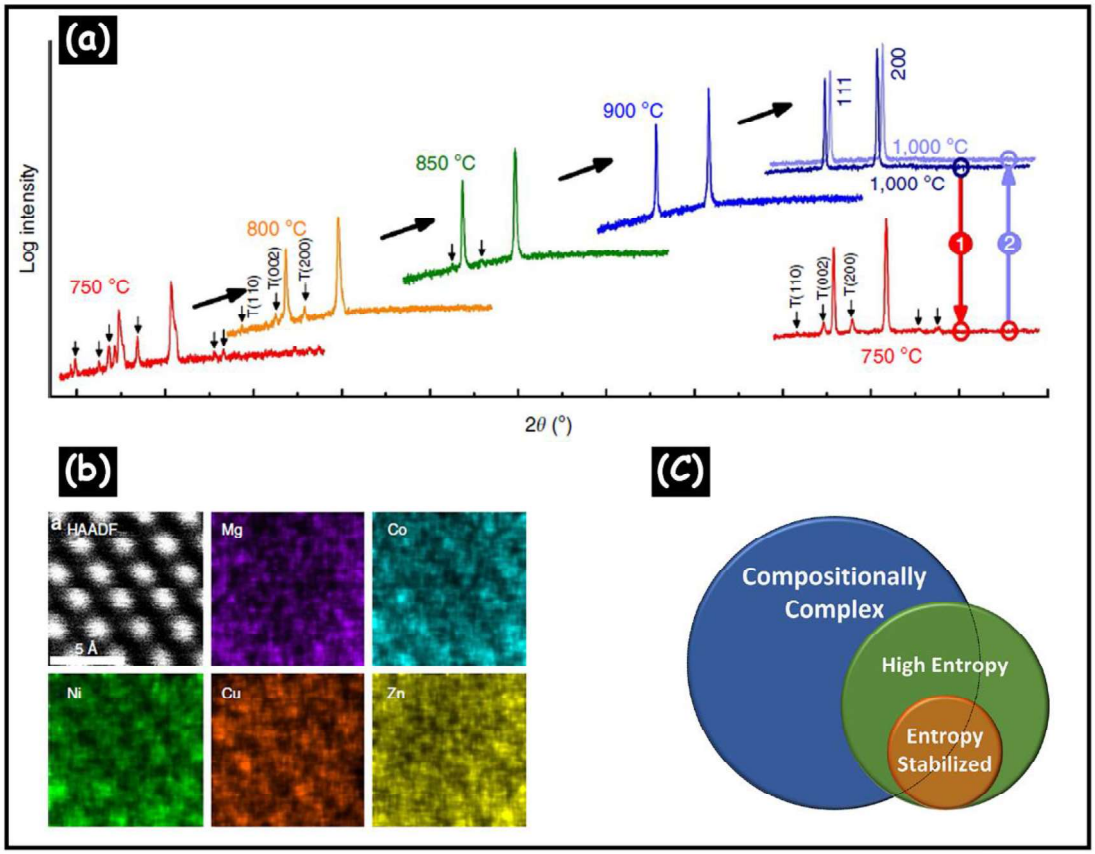

Figure 1.5: (a) Entropy driven reversible transition from multiphase to single phase (b) corresponding STEM-HAADF-EDS mapping of rocksalt HEO and (c) Venn diagram of concentrated materials [78,79].

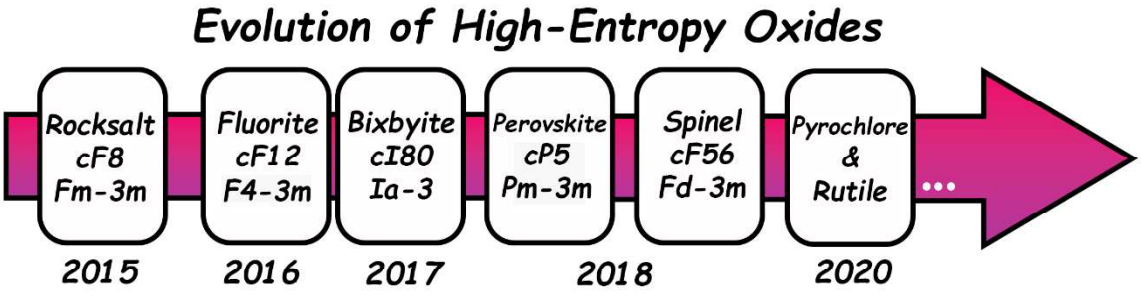

Figure 1.6: Various sub-class of HEOs with their space group and Pearson symbol.

They can have multiple sublattices for either cation or anion or both and substitution may occur in either of them, which makes calculation of configurational entropy of the system much more robust.

In addition, any ceramic system is governed majorly by ionic bonding in contrast to metallic bonding in HEAs. This makes such systems sensitive to environment and processing conditions in order to sustain their defect equilibria and net charge neutrality. Despite challenges, empirical criteria for formation of ESOs highlight the importance of similar cationic radii at specific oxidation state and coordination number, along with non-isostructuralism in at least one precursor oxide coupled with immiscibility in at least one pair of constituent binary oxides [78,83]. It is further believed that in HEOs, the presence of ordered anion-sublattice accommodates the non-stoichiometry and possible defect structure in the cation-sublattice during processing. This helps to preserve the complete disorder in the multi-cationic sublattice, allowing the formation of a homogeneous single-phase solid-solution [78-84].

1.3.1. Thermodynamics

The desire to come up with “new” and “exotic” materials is envisaged to outrun basic thermodynamic considerations for designing future HEOs [22,85]. Ideal mixing dictates that the number of components in a solid-solution does not affect the solubility of an additional component, but such systems are rare-most, if not hypothetical. In real systems, the type and nature of the additional component, its structural transformations and its pair-wise non-ideal interactions with other components determine the solubility limit. Due to ionic-covalent bonding in ceramics, long-range or short-range (LRO/SRO) ordering is believed to be the norm producing homologous series of compounds, which in turn decreases the overall configurational entropy [85,86]. Moreover, synthesis of

nanocrystalline HEOs can have huge impact arising out of contributions of surface energy to the overall free energy, which may shift the phase boundaries stabilizing certain polymorphs or altering the solubility-limit [87]. Proponents of entropic stabilization in multicomponent oxides over that of multi-principal elemental alloys, often argue in favour of the omnipresent ordered anion-sublattice, in the interstitial voids of which cations populate in a random disordered fashion and forms their own cation-sublattice [78]. The ordered oxygen-sublattice is thought to accommodate any defects arising out of pairwise interactions in the multi-cation sub-lattice. It is believed that ordered anion-sublattice framework protects the randomness or disorder in the cation sub-lattice, provided mixing (configurational) entropy is maximized by incorporating 5 or more cation species in equimolar or near equimolar proportions [82-84]. However, the physical picture might not be as straight forward as previously reasoned. This is so because there are families of oxides where the cation builds the lattice framework and anion goes to the interstitial voids instead; the most technologically relevant system is that of ceria (CeO_2) and other lanthanide-based oxides [88]. The relative size of anion and cation at a specific oxidation state and coordination environment determines their site specificity in the lattice [89]. Apart from that, there could be more than one cation and/or anion sublattices dictated by order, disorder or both. Processing conditions, especially partial pressure of the gas being purged can significantly alter the local defect structure in either of the sublattice along with enriched/deficient sub-lattice in order to maintain net charge neutrality [89]. This introduces complexity in the already oversimplified entropy of mixing term in the free energy equation, which is frequently overlooked. In the literature of CoCuMgNiZn HEO, there are few reports on the possible co-existence of allied spinel phase in minor fraction apart from defect microstructure and Jahn-Teller distortions caused by Cu^{+} and/or Co^{3+} ions in the phase evolution process [90-92]. Moreover, in the x-ray diffraction signatures of the

HEO, the intensity ratios do not match with the ideal cF8 (Fm-3m) crystal structure of rocksalt. Apart from that, systematic shoulder peaks at roughly half the intensity of accompanying Bragg peaks could be observed in sintered and quenched HEOs, which has been attributed to $K\alpha_{II}$ excitation [84]. However, this does not appear to be very convincing since wavelengths of the Kα doublets differ in the 3rd place of decimal which results to angular deviation in the second place of decimal of 2θ, but experimentally observed difference in angular disposition are several times higher. Documentation regarding stability of the entropy stabilized single-phase in CoCuMgNiZn ESO as well as other HEOs is quite scarce in literature so far. Although few theoretical modelling and simulation, along with in-situ heating and calorimetry experiments have explored the stability of the phases, however for very limited exposure times, which may not be comparable to the kinetics of such chemically complex multicomponent systems [78-84]. In this context, thermodynamic stability is a pressing issue and it is worth re-visiting this fundamental aspect with the help of Figure 1.7. Assuming the solid in Figure 1.7 to be iron, which can exist in all three solid, liquid and gaseous states, it is known for a fact that enthalpy of liquid iron will always be more than that of solid iron, as entropy too of liquid iron will always be greater than that of its solid. However, below the melting point, a state of matter with lower enthalpy or entropy is more stable, but in transforming to liquid above its melting point makes both the enthalpy and entropy higher. Thus, a generalized statement cannot be made that a phase with lower enthalpy or higher entropy is always stable or shall remain to be stable. Above the melting point, the liquid has lower free energy at all temperatures than the solid, and below the melting point, the solid always has lower free energy. To summarize, solid is always stable below T_m while liquid is always stable above T_m, as both have lower free energy. This is the reason that free energy (G) is the only thermodynamic descriptor that is used as a single stability criterion.

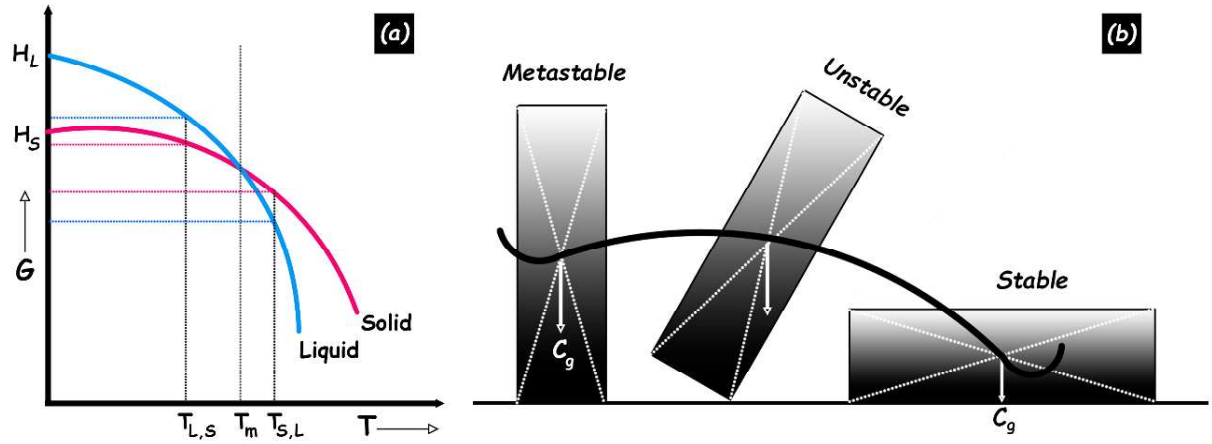

Figure 1.7: (a) G vs T plot of a solid and its liquid at constant pressure, where the slope of the curves gives entropy and its intercept the enthalpy while (b) is the schematic demonstration of local minima separated by activation barrier in the energy landscape of a mechanical object as it falls.

Therefore, a phase with higher configurational entropy but higher free energy is less stable than a phase with lower configurational entropy but lower free energy. The manifestation of enthalpic penalties combined with maximizing randomness in the multi-cationic sublattice in multicomponent oxides shall be demonstrated throughout this thesis.

1.3.2. Structure

Metallurgists are traditionally interested in impure materials, be it alloyed or doped. They are also most interested in deciphering the crystal structure and exploring the microstructure of alloys, compounds and composites. It is well established that composition is profoundly co-related with both microstructure and crystal structure of any material and vice-versa, which in turn dictates the material properties [93,94]. Hence, understanding the crystal and microstructure paves the path for engineering them to extract better material performance, consequently innovating materials design in general. Majority of ceramic crystal structures are based on either FCC or HCP close-packing of one type of ion(s) while the other type of ion(s) occupies specific sets of interstitial sites. The rocksalt (MO) crystal structure, having NaCl as the prototype, forms by mutual interpenetration of multiple cubic

sub-lattices. This results in the bigger Cl^- ions to build up the lattice framework with motifs at (0,0,0), (1/2,1/2,0), (1/2,0,1/2), (0,1/2,1/2) and the smaller Na^+ ions to fit in the octahedrally located voids at (1/2,1/2,1/2), (0,0,1/2), (0,1/2,0), (1/2,0,0) [93,94]. The space group becomes Fm-3m and Pearson symbol cF8. Between any two close-packed layers of anions, a hexagonal array of cations with identical periodicity can be visualized. A model structure with edge-sharing MO_6 octahedra is shown in Figure 1.8, with inset depicting the maximum radius of the ionic species occupying the octahedral voids without any distortion. For FCC close-packed systems, the motifs when approximated as hard spheres touch along the close-packed directions i.e. <110> resulting in:

$$\mathbf{4r = \sqrt{2}a} \qquad \textbf{(i)}$$

$$\mathbf{^{max}R_v = (\sqrt{2}-1)r} \qquad \textbf{(ii)}$$

Where 'a' depicts the lattice parameter of the cubic structure, 'r' is the ionic radius of Cl^- at six-fold coordination and '^{max}Rv' is the maximum ionic radius of the smaller Na^+ ions that can snugly fit in the octahedral void. Solving equations (i) and (ii) yields:

$$\mathbf{^{max}R_v = 0.146a} \qquad \textbf{(iii)}$$

Since the formation and stability of all ionic compounds are governed by Pauling's rules, it demands that the radius ratio (r_c/r_a) must lie between 0.414-0.732 for a rocksalt structure [20]. Transitioning to spinel crystal structure, it is a 2x2x2 supercell where anions decorate the overall FCC lattice framework while cations partially fill up both the octahedral and tetrahedral voids. Spinels have general formula of AB_2O_4 where cations in +2 oxidation states prefer filling half of the octahedral voids whereas cations in +3 oxidation states prefer to fill out one-eighth of the tetrahedral voids [93-95]. There could be inverse spinel structure with different site-specificity of the cations or there could be mixed spinel with random occupation of cations.

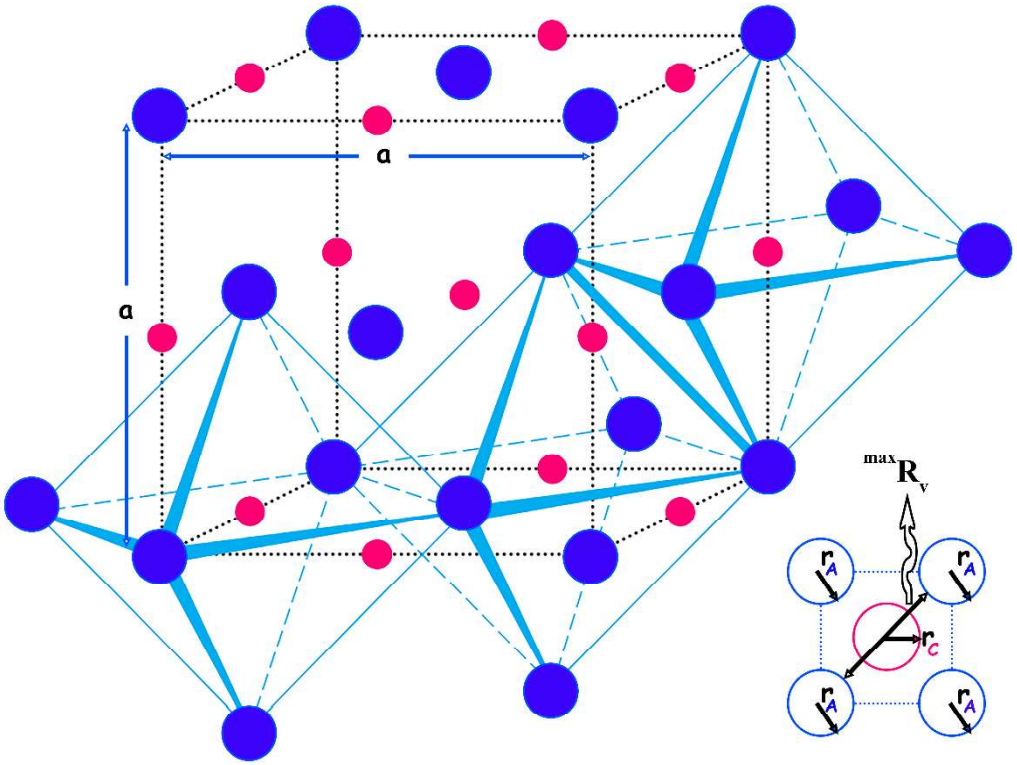

Figure 1.8: A typical rocksalt prototype structure with anions (marked in blue) decorating the fcc lattice positions and cations (marked in red) occupying the octahedral voids. Three edge-sharing six-fold coordination polyhedras are depicted for clarity.

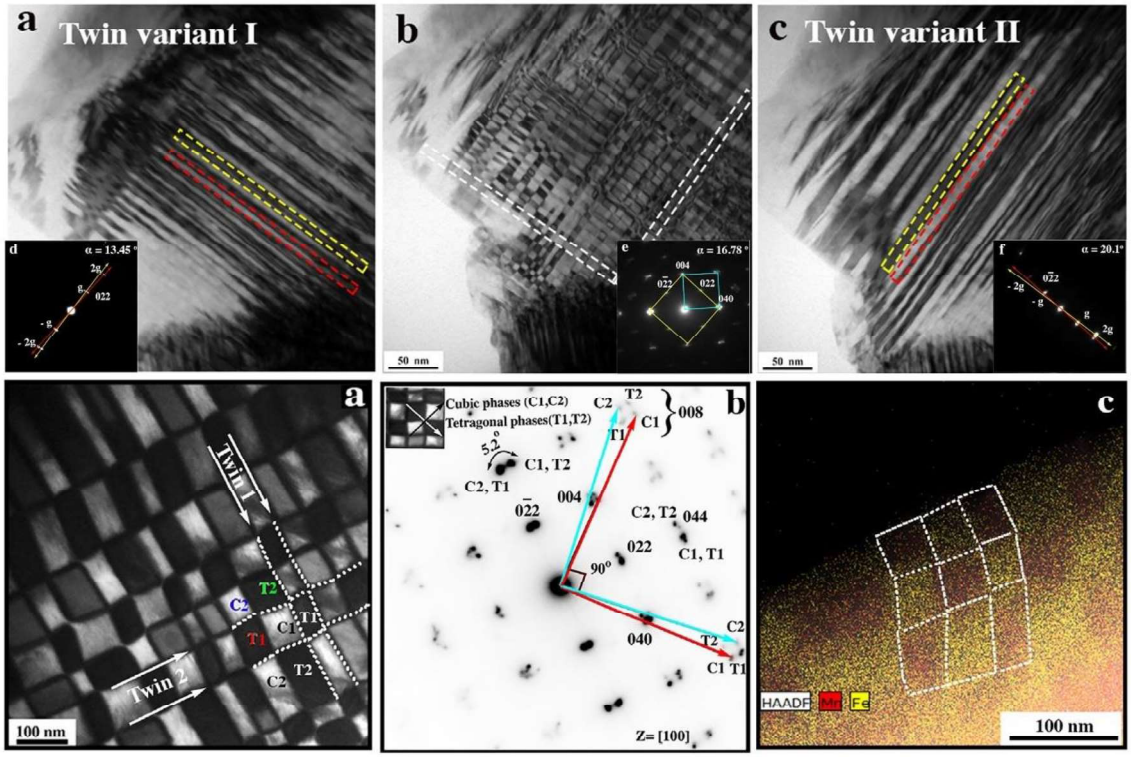

Figure 1.9: Recurrent compositional phase separation leading to a chessboard-like microstructure in CoFeMn medium entropy oxide characterized by spinel structure [103].

The cubic spinel is designated by Fd-3m space group and cF56 Pearson symbol. This is the highest symmetry group of cubic spinel, while other polymorphs of the phase have lower symmetry elements [95]. Apart from that, both cubic rocksalt and cubic spinel are amenable to distortions in the cubic crystal structure leading to tetragonal, orthorhombic, rhombohedral and even monoclinic variants [96-99]. It is perhaps important to further realize that the spinel mineral ($MgAl_2O_4$) is a highly ordered normal spinel which forms under extreme heat and pressure over geological time spans. Thus, lab or industry synthesized $MgAl_2O_4$ will always be disordered to certain degree, which holds good for most of the spinel forming materials that has been synthesized or ever will be [94].

Polytypism is another well documented phenomenon closely related to polymorphism in ceramics, although the variants of a particular structure only differ with respect to the stacking sequence of intermediate 2-D layers [94]. Complex disposition of anti-phase boundaries (APBs) has been witnessed in simple parent structure types [97]. Moreover, phase separation within monophasic transition metal oxides has been well explored by Rao and his co-workers [100,101]. They are mostly driven by the competition between charge localization and delocalization which has contrasting magnetic and electric properties. Such kinds of phase separation were mostly recorded during early 2000's in cuprates and manganates with length scale of phase separation lying anywhere between 1-200 nm [100-102]. Couple of decades later, Pal et. al successfully demonstrated chessboard-like (CB) microstructure in multicomponent CoFeMn and CoFeGaMnZn spinel oxide through recurrent compositional phase separation and cross-penetration of twin variants, shown in Figure 1.9 [103,104]. The sequence of phase transformation events leading to nano CB microstructure has been explained in light of twinning-induced, pseudo-spinodal segregation of ionic species. Crystallographic model of evolution of CB microstructure based on irregular octahedra's face-sharing with one another along elastically soft <022>

directions has also been put forth. During the same time, Singh et al. reported type-I and type-II rhombohedral distortions in layered rocksalt structured Li(Ni,Mn)O cathode material [105]. Non-cubic distortions to binary/ternary cubic rocksalt and cubic spinel is also reported [110]. Apart from chemical modulation, phase separation and ordering, early works of Tilley, Anderson and Hyde during 1970's reveal extensive planar fault mediated exotic structures in various metal oxides [106-109]. Earlier it was believed that non-stoichiometry in metal oxides is structurally accommodated by point defects like in $Fe_{1-n}O$, $TiO_{1\pm n}$, $VO_{1\pm n}$ among others [110]. Later it was found that most often than not, such changes due to anion/cation ratio is accommodated by planar faults or intergrowth structures like in reduced WO_3, TiO_2, Nb_2O_5 and many others [106-109].

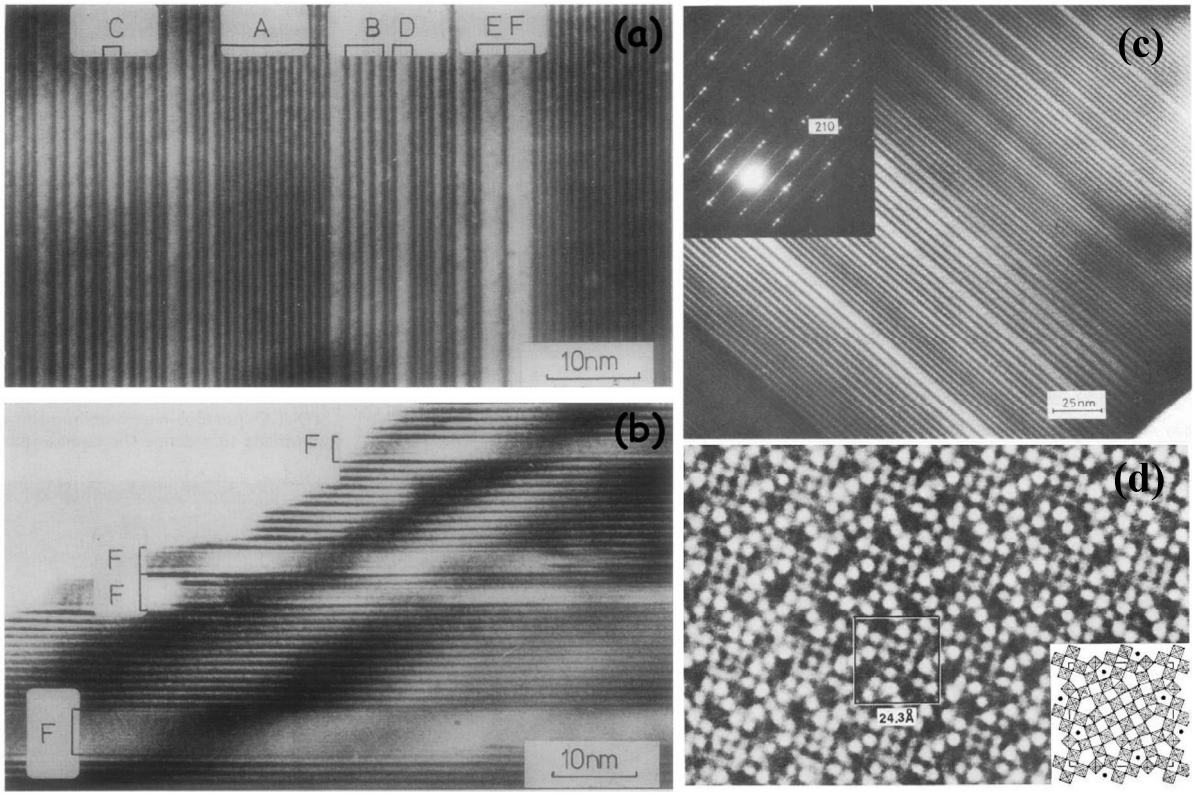

Figure 1.10: (a) Disordered $Sr_3Ti_2O_7$ crystal with phase intergrowths from varying stoichiometries, (b) intergrowth of stable $SrTiO_3$ (c) TEM BF image of disordered faults on (210) planes of doped TiO_2 with corresponding electron diffraction pattern at the inset and (d) phase-contrast image of $2Nb_2O_5$, $7WO_3$ [108,109].

They also demonstrated special tiling structures at atomic scale due to mutual rotation between domains in geometrically frustrated spinels, perovskites and spinelloids such as $CaFe_2O_4$, $BaFe_{12}O_{19}$, $SrTi_2O_3$ among others [106-109,111]. The process of interaction of planar defects leading to ordering, clustering or elimination of point defects is known as "crystallographic shear" (CS) and the trace of such planes are termed CS planes. The micrographs of such extensive faulted structures have been depicted in Figure 1.10 along with corresponding streaked electron diffraction pattern and high-resolution phase-contrast image [108,109].

1.3.3. Properties

1.3.3.1. Mechanical properties

Extensive research on HEOs in less than a decade has made them a popular choice for its use in several applications along with scope for further enhancement. The rutile (TiO_2 prototype) structure exhibits highest hardness and elastic modulus among all the HEO family of structures [112]. The fluorite (CaF_2 prototype) HEOs generally show greater hardness than pyrochlore HEOs [113]. Due to the inherent oxidation and corrosion resistance, HEOs are also being fabricated in thick and thin films for environmental and abrasive coatings in structural components. Al_2(CoCrCuFeNi)O and (AlCrTaTiZr)O have shown the highest hardness in all of the existing oxide coatings at ~22 and ~20 GPa respectively [114]. Low thermal conductivity coupled with sluggish grain-growth kinetics have made HEOs viable options for refractory applications as well as thermal barrier coatings (TBCs) for aero-engines and gas-turbines [112]. Moreover, there remains tremendous scope for engineering the composition, phase and microstructure of such HEOs in order to explore materials with very low or negative thermal expansion coefficients [112-114].

1.3.3.2. Functional properties

Transition metal oxides have long been explored for their favourable polarization and charge-lattice coupling response [115]. Chemical modulation has been intrinsically linked with the phase stability for desirable ferroelectric, dielectric and piezoelectric response [115]. In this context, MCOs/ESOs/HEOs have emerged as attractive candidates for enhanced properties owing to the entropic stabilization of disordered solid-solution phase(s) in them [112-114]. It is believed that global-scale disorder in materials may give rise to polar nanoregions (PNR) and its coupling with lattice phonons propels the property as a relaxor ferroelectric material [112]. Additionally, geometric frustration may induce local distortions which enhances dielectric and piezoelectric response [114]. Few research groups have shown that (CoCuMgNiZn) rocksalt ESO exhibit structural tunability upon varying the composition, owing to Jahn-Teller distortions induced by Cu- and/or Co-ions, which results in high dielectric constants and favourable catalytic activity [92,116]. It has also been demonstrated to possess superior lithium-storage properties due to tunable pseudocapacitive contributions [117]. Relaxor-like characteristics have been reported for Ba(ZrSnTiHfNb) perovskite HEO [112]. (LaPrNdSmEu)NiO_3 HEO have been found to go through a low temperature metal-insulator transition, attributed to geometric distortions arising out of coordinated octahedra tilting [80]. Fluorite (CeLaPrSmY)O_2 have demonstrated that the band gap and crystal structure can be tuned via oxygen stoichiometry due to the hybridization of oxygen and rare earth elements, which in turn may be developed for scintillator and laser applications [81]. Furthermore, double-exchange and super-exchange phenomena renders HEOs with tunable properties like ferro-/anti-ferro-, ferri-/anti-ferri- and diamagnetism [118]. Ferrite based spinel HEO like (CoCuMgNiZn)Fe_2O_4 have shown soft magnetic character with coercive field of ~100 Oe, whereas, chromite-based spinel HEOs like (CoCuFeMgNi)Cr_2O_4 have recorded coercive field as high as 1 T

[112]. HEO ferrites are also promising candidates as magnetic insulators with good quality surface for its application in spintronics and nonvolatile memory devices [112-114].

1.3.4. Fields of application

The field of high entropy ceramics (HECs) blossomed since the first ever reported HEO in 2015 [78,80]. They mainly caught attention of researchers because of their remarkable properties, apart from debatable schools of thought so far their phase formation, stability and microstructural evolution is concerned [81, 85-87]. Focusing on the properties, HEOs have been reported to be promising candidates in various fields of application, an overall schematic of which is given in Figure 1.11. Understanding and engineering charge transport mechanisms in HEOs offer promising avenues for exploring enhanced properties, especially as electrode material for secondary-ion batteries and fuel cells [112-114].

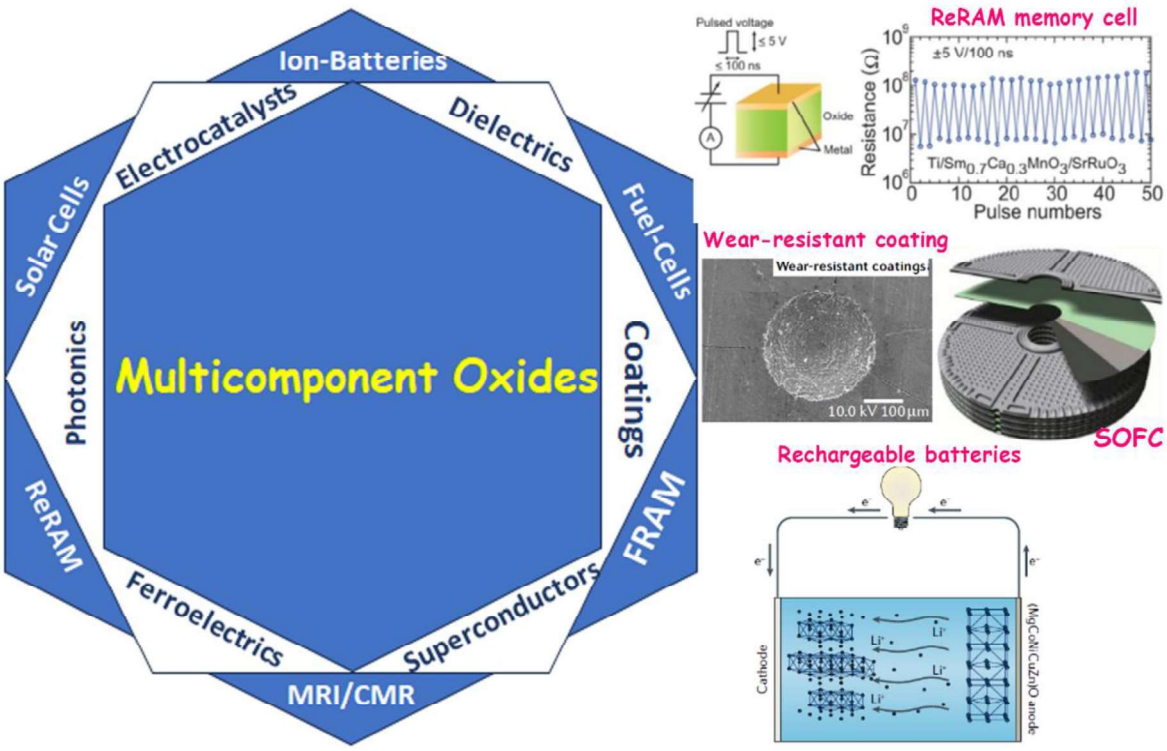

Figure 1.11: Fields of application for HEOs reported so far.

HEOs have already become promising candidates as anode material, cathode material as well as solid-state electrolyte for Li-ion batteries [119,120]. Soon after the first HEO was successfully synthesized, Berardan and coworkers reported room temperature superionic conductivity of Li-ions (> 10^{-3} S/cm) and fast mobility of Na-ions (> 10^{-6} S/cm) in $(MgCoNiCuZn)_{1-x-y}Ga_yA_x$ (where A=Li, Na, K) HEO, significantly exceeding the generally used lithium phosphorous oxy-nitride solid-state electrolyte [117]. They also reported colossal dielectric constant for doped rocksalt-based HEOs, which have the potential to serve as high-*k* dielectric materials [116].

(MgCoNiCuZn) HEO has also demonstrated good charge cycling response and very high specific capacities. The currently favoured anode material is graphite with a capacity of ~360 mAh/g [112]. Rocksalt type high entropy oxyfluorides have also been explored as cathode material for Li-ion batteries and they have delivered specific energies up to ~307 mAh/g, with scope for further improvement [119]. An equimolar hexanary HEO has been reported to show ~40% increase in capacity and energy density as cathode material than its constituent lower-order oxides [112]. Coin cells fabricated with (MgCoCuNiZn)O as polysulfide anchor show competitive reversible capacity, excellent cycling stability and low-capacity decay for its use in lithium-sulfur batteries [120].

Multi-cationic HEOs have compositional freedom which translates to substantial electronic structure and coordination environment tunability, that makes them ideal candidates as catalysts [121]. (FeNiCoCrMn)-layered glycerate HEO have shown rapid transport of reactants to the material while providing additional catalytic active sites [121]. The use of $(FeMgCoNi)O_{1.2}$ poly-cationic oxide (PCO) has demonstrated a significant reduction of temperature under which efficient hydrogen evolution reaction occurs via two-step thermochemical water-splitting [122]. HEOs have also shown promise as catalytic booster for oxidative desulphurization of diesel [112]. Mesoporous $(MgCoNiCuFe)_x$-Al_2O_3 have

reported against CO oxidation and CO_2 hydrogenation and have showed negligible degradation after 48h along with superior sulfur tolerance to CuO-Al_2O_3 [113]. Spinel-based HEOs are further being exploited for efficient oxygen evolution reaction (OER) and hydrogen evolution medium (HER) from electrochemical water-splitting [123]. Rocksalt-based HEOs on the other hand have been found to exhibit long-range antiferromagnetic ordering below Neel temperature of ~113 K, suitable for its use in memory devices [124,125].

It has been demonstrated that local disorder in ionic charge can further reduce the thermal conductivity of HEOs without compromising on the mechanical stiffness. Equimolar (MgNiCoCuZnSb) HEO has shown the lowest conductivity of ~1.4 W/mK among similar class of materials [126]. Perovskite-based (BaCaLaPbSr)TiO_3 HEO have shown ~5 times reduction in thermal conductivity compared to $SrTiO_3$, with figure of merit over 0.2 [112]. Thin films of hexanary Ba(ZrSnTiHfNb)O_3 HEO with perovskite structure has recorded thermal conductivity of ~0.55 W/mk, which is an order of magnitude lower than binary or ternary perovskites [114]. High entropy niobates or zirconates have become promising candidates for thermal and environmental protection applications, owing to their very low thermal conductivity along with uncompromised mechanical rigidity [80]. (AlCrTaTiZr) HEO has been reported extremely high hardness values of ~22 GPa as well as exceptional wear resistance [81]. $(LaNdSmEuGd)_2Ti_2O_7$ HEO with pyrochlore structure has been reported to withstand up to 5 times the thermal cycling as $La_2Zr_2O_7$ can withstand [112]. Similar HEOs are also known to have reduced leaching rates compared to its lower-order derivatives, and consequently are being considered for managing nuclear waste [112].

1.4. Objectives of the thesis

- Systematic partial substitution of one or more cationic species with other ones is theoretically known to keep the configurational entropy of the whole equimolar mixture intact [72]. However, this simple logical assumption has been debunked in the recent past in HEA literature [75-77]. Thorough investigations with a clear understanding in this regard is yet to be realized in HEOs and it has been taken up in this research.
- In principle, HEOs should crystallize in a single-phase with random and homogeneous distribution of ions across all length scales [78]. However, that is perhaps not the scenario. The initial goal of the current research has been to synthesize and characterize equimolar binary, ternary, quaternary derivatives of the equimolar quinary rocksalt and spinel HEOs (CoCuMgNiZn)O and $(CoCrFeMnNi)_3O_4$ respectively by systematic partial substitution. The random distribution of multiple cations forming simple solid-solution phase with rocksalt or spinel structure has been explored throughout this thesis, in an attempt to understand the mechanism behind the entropic stabilization in HEOs.
- Thermodynamic stability of HEOs has been a pressing issue since its inception and it has hardly been tackled in literature [85,86]. The consequences of prolonged heat treatments on the phase stability and microstructural evolution in various multicomponent oxides have been examined through systematic diffraction, electron microscopy and spectroscopy experiments. In this regard, XRD, SEM-SE/BSE imaging, SEM-XEDS analytical mapping, TEM imaging and SAED techniques have been exhaustively utilized.
- Another primary objective behind carrying out the current research revolves around the manifestation of lattice strain due to geometric frustration in both the sub-lattices in HEOs. Additionally, the effect of volumetric strain due to competition between multiple cations with non-ideal interactions among them has been explored. There is also a

possibility of interfacial strain build-up due to local structural modulation or intergrowth of correlated second phases, which too has been investigated throughout this research work.

- Presence of secondary phase(s), evolution of defect microstructure, chemical or structural modulation at sub-micron length scales and diffusion-assisted reconstructive phase transformations have been thought of in HEO literature [91,92]. However, direct evidences for such schools of thought are scarce. It has been carefully examined throughout the research work carried out in this thesis.
- HEOs have been reported to outperform its monolithic counterparts by leaps and bounds in several applications so far [112]. The enhanced properties are often attributed to the synergistic effect arising out of high configurational entropy [113,114]. However, a sound picture of structure-property correlation is missing. The research work in this thesis explores the catalytic activities of several multicomponent oxides for efficient evolution of oxygen and hydrogen from electrochemical water-splitting experiments. The properties have been correlated with the crystal structure, its deviation from ideality, relative phase fractions and segregation of redox active species.
- In order to arrive at a holistic picture, the popular 'materials tetrahedron' strategy has been adopted throughout this thesis. It is schematically represented in Figure 1.12. Synthesis and processing of various MCOs/ESOs/HEOs have been characterized at the microstructural and crystal structure length scales, and a correlation is established with the obtained properties. Modeling and simulation techniques have also been employed to validate the experimental findings.

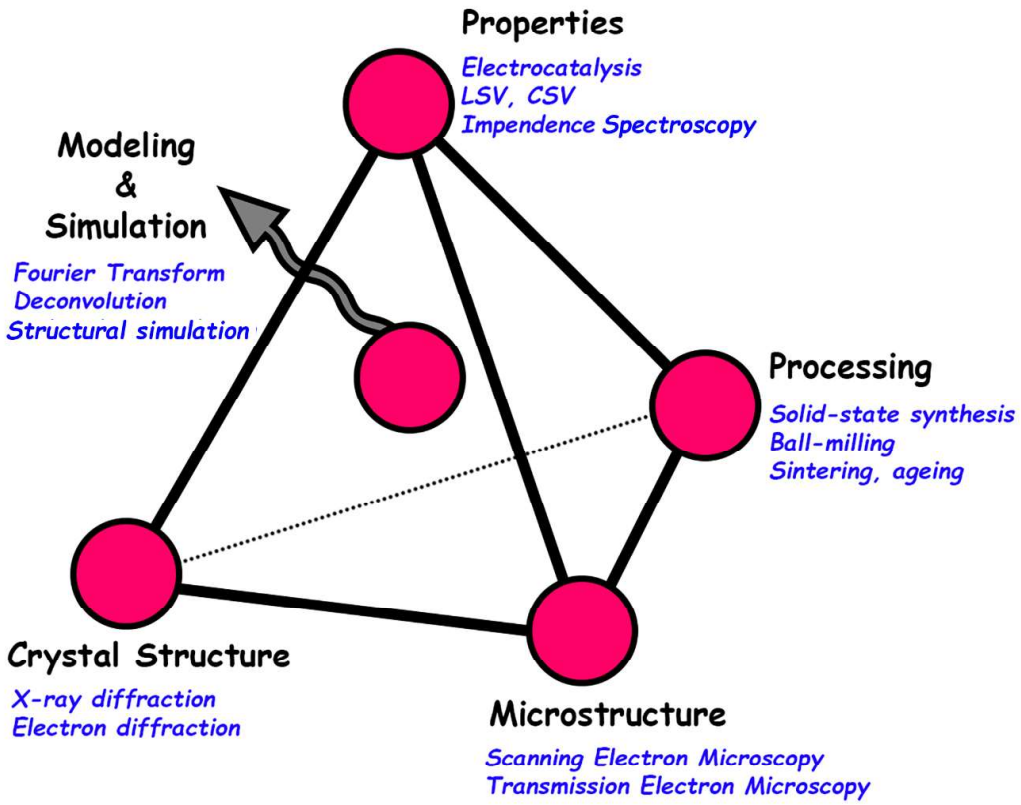

Figure 1.12: Materials tetrahedron describing the correlative interconnection between processing and properties via characterization and computation after a suitable composition is identified. This approach has been followed throughout the thesis and implemented on several multicomponent oxides.

1.5. Reference

1. C. Liu, F. Li, L. P. Ma, H. M. Cheng, Advanced materials for energy storage, Adv. Mater., 2010, 22, E28-E62
2. B. C. H. Steele, A. Heinzel, Materials for fuel-cell technologies, Nature, 2001, Vol. 414, 345-352
3. X. Yu, Z. Tang, D. Sun, L. Ouyang, M. Zhu, Recent advances and remaining challenges of nanostructured materials for hydrogen storage applications, Prog. Mater. Sci., 2017, Vol. 88, 1-48
4. A. S. R. Bati, M. Batmunkh, J. G. Shapter, Emerging 2D layered materials for perovskite solar cells, Adv. Energy Mater., 2019, 1902253 (21 pages)

5. J. Knaster, A. Moeslang, T. Muroga, Materials research for fusion, Nature Physics, 2016, Vol. 12, 424-434
6. Y. Liu, X. Zhang, Metamaterials: a new frontier of science and technology, Chem. Soc. Rev., 2011, Vol. 40, 2494-2507
7. N. I. Zheludev, Y. S. Kivshar, From metamaterials to metadevices, Nature Materials, 2012, Vol. 2, 917-924
8. Sir C. V. Raman, The Indian musical drums, Proc. Ind. Acad. Sci., A, 1934, Vol. 1 (II) (14 pages)
9. S. J. Zinkle, J. T. Busby, Structural materials for fission & fusion energy, Materials Today, 2009, Vol. 12 (11), 12-19
10. K. Kumar, J. Bandi, L. R. Tenneti, The Indian steel industry: Growth, challenges and digital disruption, PwC India, 2019 (28 pages)
11. J. A. Mathews, A Silicon Valley of the East: Creating Taiwan's semiconductor industry, California Management Review, 1997, Vol. 39 (4) (30 pages)
12. A. C. Reardon, Discovering Metals: A historical overview, Metallurgy for Non-Metallurgist, 2011, Vol. 74 (2) (12 pages)
13. R. F. Mehl, A Brief History of the Science of Metals, The Maple Press Company, USA, 1948 (88 pages)
14. B. Cohen, The Eighteenth-Century Origins of the Concept of Scientific Revolution, Journal of the History of Ideas, USA, 2014 (33 pages)
15. R. W. Cahn, Alloy design: a historical perspective, Proc. Indian Acad. Sci., 1980, Vol. 3 (4), 255-260
16. S. Ghosh, J. Basu, D. Ramachandran, E. Mohandas, M. Vijayalakshmi, A unified approach to phase and microstructural stability for Fe-ETM alloys through Miedema's model, Intermetallics, 2012, Vol. 23, 148-157

17. W. H. Rothery, The freezing points, melting points and the solubility limits of the alloys of silver and copper with the elements of B-subgroup, Philosophical Transactions of the Royal Society of London, 1933, Vol. 223
18. A. Inoue, Stabilization of metallic supercooled liquid and bulk amorphous alloys, Acta Mater., 2000, Vol. 48, 279-306
19. D. G. Pettifor, The structure of binary compounds I: Phenomenological structure maps, J. Phys. C: Solid State Physics, 1986, Vol. 19 (3), 285-313
20. L. Pauling, The principles determining the structure of complex ionic crystals, J. Am. Chem. Soc., 1929, Vol. 51 (4), 1010-1026
21. S. P. Pandey, V. Singh, The importance of engineering materials in present world, Int. J. Sci. & Res., 2017, Vol. 6 (3), 433-441
22. W. Steurer, Single-phase high-entropy alloys: A critical update, Materials Characterization, 2020, Vol. 162, 110179
23. T. W. Liao, G. Li, Metaheuristic-based inverse design of materials: A survey, J. Materiomics, 2020, Vol. 6, 414-430
24. C. Y. Lee, C. Y. Jui, A. C. Yeh, Y. J. Chang, W. J. Lee, Inverse design of high entropy alloys using a deep interpretable scheme for materials attribution analysis, J. Alloys Comp., 2024, Vol. 976, 173144 (12 pages)
25. J. Bierman, Science and society in the *New Atlantis* and other renaissance utopias, PMLA, 1963, Vol. 78 (5), 492-500
26. W. R. Nitske, The Life of Wilhelm Conrad Rontgen, Discoverer of the X-ray, University of Arizona Press, 1971 (355 pages)
27. E. Ruska, The development of the electron microscope and of electron microscopy, Reviews of Modern Physics, 1987, Vol. 59 (3) (24 pages)

28. P. W. Hawkes, J. C. H. Spence, Science of Microscopy, Vol. I, Springer, USA, 2008, 98765432
29. D. B. Williams, C. B. Carter, Transmission Electron Microscopy: A Textbook for Materials Science, Springer, USA, 2009, Edition 2, Vol. I-IV (779 pages)
30. H. Okamoto, T. B. Massalski, Guidelines for binary phase diagram assessment, J. Phase Equilibria, 1993, Vol. 14 (3), 316-335
31. R. Kanno, M. Tsujii, K. Hanya, K. Matsuoka, T. Tominaga, F. Ozaki, Steels, Steel Products and Steel Structures Sustaining Growth of Society (Infrastructure Field), Nippon Steel Technical Report, No. 101, 2012, 57-67
32. L. Gardner, The use of stainless steel in structures, Prog. Struct. Eng. Mater., 2005, Vol. 7, 45-55
33. H. K. D. H. Bhadeshia, Steels for bearings, Progress in Materials Science, 2012, Vol. 57, 268-435
34. Y. Wei, Y. Li, L. Zhu, Y. Liu, X. Lei, G. Wang, Y. Wu, Z. Mi, J. Liu, H. Wang, H. Gao, Evading the strength-ductility trade-off dilemma in steel through gradient hierarchical nanotwins, Nat. Commun., 2014, Vol. 5, 3580, 1-8
35. J. Rosler, O. Nath, S. Jager, F. Schmitz, D. Mukherji, Fabrication of nanoporous Ni-based superalloy membranes, Acta Mater., 2005, Vol. 53, 1397-1406
36. H. Choe, D. C. Dunand, Synthesis, structure, and mechanical properties of Ni-Al and Ni-Cr-Al superalloy foams, Acta Mater., 2004, Vol. 52, 1283-1295
37. I. Gurrappa, Characterization of titanium alloy Ti-6Al-4V for chemical, marine and industrial applications, Materials Characterization, 2003, Vol. 51, 131-139
38. K. K. Mccabe, S. L. Sass, The initial stages of the omega phase transformation in Ti-V alloys, Philos. Mag., 1971, Vol. 23, 184, 957-970

39. S. K. Sikka, Y. K. Vohra, R. Chidambaram, Omega phase in materials, Prog. Mater. Sci., 1982, Vol. 27, 245-310
40. C. Ghosh, J. Basu, D. Ramachandran, E. Mohandas, Phase separation and ω transformation binary V-Ti and ternary V-Ti-Cr alloys, Acta Mater., 2016, Vol. 121, 310-324
41. A. Devaraj, S. Nag, R. Srinivasan, R. E. A. Williams, S. Banerjee, R. Banerjee, H. L. Fraser, Experimental evidence of concurrent compositional and structural instabilities leading to ω precipitation in titanium-molybdenum alloys, Acta Mater., 2012, Vol 60, 596-609
42. W. H. Rothery, The Structure of Metals and Alloys, Nature, 1936, Monograph and Report Series No.1, Vol. 38, London Institute of Metals
43. Y. M. Zhang, S. Yang, J. R. G. Evans, Revisiting Hume-Rothery's rules with artificial neural networks, Acta Mater., 2008, Vol. 56, 1094-1105
44. U. Mizutani, H. Sato, T. B. Massalski, The original concepts of the Hume-Rothery rule extended to alloys and compounds whose bonding is metallic, ionic, or covalent, or a changing mixture of these, Prog. Mater. Sci., 2021, Vol. 120, 100719
45. D. Turnbull, Theory of catalysis of nucleation by surface patches, Acta Metallurgica, 1953, Vol. 1 (1), 8-14
46. P. Duwez, Metastable phases obtained by rapid quenching from the liquid state, Progress in Solid State Chemistry, 1967, Vol. 3, 377-400
47. Joysurya Basu, Glass Forming Ability and Stability: Bulk Zr-based and Marginal Al-based Glasses, PhD Thesis, 2004, Indian Institute of Science©, Bangalore, India
48. J. Basu, S. Ranganathan, Crystallisation in Al-ETM-LTM-La metallic glasses, Intermetallics, 2004, Vol. 12, 1045-1050

49. J. Basu, S. Ranganathan, Glass-forming ability and stability of ternary Ni-early transition metal (Ti/Zr/Hf) alloys, Acta Mater., 2008, Vol. 56, 1899-1907
50. J. Basu, D. V. Louzguine, A. Inoue, S. Ranganathan, Synthesis and devitrification of glassy Zr-Ti-Ni and Zr-Hf-Ni ternary alloys, Journal of Non-Crystalline Solids, 2004, Vol. 334&335, 270-275
51. H. Tanaka, Possible resolution of the Kauzmann paradox in supercooled liquids, Physical Review E, 2003, Vol. 68, 011505
52. A. Inoue, Stabilization of metallic supercooled liquid and bulk amorphous alloys, Acta Mater., 2000, Vol. 48, 279-306
53. W. L. Johnson, Thermodynamic and kinetic aspects of the crystal to glass transformation in metallic materials, Prog. Mater. Sci., 1986, Vol. 30, 81-134
54. A. Inoue, Amorphous, nanoquasicrystalline and nanocrystalline alloys in Al-based systems, Prog. Mater. Sci., 1998, Vol. 43, 365-520
55. A. Inoue, A. Takeuchi, Recent development and application products of bulk glassy alloys, Acta Mater., 2011, Vol. 59, 2243-2267
56. G. V. S. Sastry, C. Suryanarayana, A new ordered phase in the Al-Pd system, Mat. Res. Bull., 1978, Vol. 13, 1065-1070
57. G. V. S. Sastry, V. V. Rao, P. Ramachandrarao, T. R. Anantharaman, A new quasi-crystalline phase in rapidly solidified Mg_4CuAl_6, Scripta Metallurgica, 1986, Vol. 20, 191-193
58. N. K. Mukhopadhyay, S. Ranganathan, K. Chattopadhyay, On the short-range order in Al-Mn quasicrystals during low-temperature ageing, Philos. Mag. Lett., 1987, Vol. 56 (4), 121-127

59. N. K. Mukhopadhyay, G. N. Subbanna, S. Ranganathan, K. Chattopadhyay, An electron microscopic study of quasicrystals in a quaternary alloy $Mg_{32}(Al,Zn,Cu)_{49}$, Scripta Metallurgica, 1986, Vol. 20 (4), 525-528

60. B. Cantor, I. T. H. Chang, P. Knight, A. J. B. Vincent, Microstructural development in equiatomic multicomponent alloys, Mat. Sci. Eng. A, 2004, 375-377, 213-218

61. J. W. Yeh, S. K. Chen, S. J. Lin, J. Y. Gan, T. S. Chin, T. T. Shun, C. H. Tsau, S. Y. Chang, Nanostructured high-entropy alloys with multiple principal elements: Novel alloy design concepts and outcomes, Advanced Engineering Materials, 2004, Vol. 6 (5), 299-303

62. I. Ansara, N. Dupin, H. L. Lukas, B. Sundman, Thermodynamic assessment of the Al-Ni system, Journal of Alloys and Compounds, 1997, Vol 247, 20-30

63. J. Q. Guo, K. Ohtera, Microstructures and mechanical properties of rapidly solidified high strength Al-Ni based alloys, Acta Mater., 1998, Vol. 46 (11), 3829-3838

64. N. K. Mukhopadhyay, High entropy alloys: a renaissance in physical metallurgy, Current Science, 2015, Vol. 159 (4), 665-667

65. S. Ranganathan, Alloyed pleasures: Multimetallic cocktails, Current Science, 2003, Vol. 85 (10), 1404-1406

66. F. Otto, Y. Yang, H. Bei, E. P. George, Relative effects of enthalpy and entropy on the phase stability of equiatomic high-entropy alloys, Acta Mater., 2013, Vol. 61, 2628-2638

67. Y. Zhang, T. T. Zuo, Z. Tang, M. C. Gao, K. A. Dahmen, P. K. Liaw, Z. P. Lu, Microstructures and properties of high-entropy alloys, Prog. Mater. Sci., 2014, Vol. 61, 1-93

68. J. M. Torralba, P. Alvaredo, A. G. Junceda, High-entropy alloys fabricated via powder metallurgy: a critical review, Powder Metallurgy, 2019, Vol. 62 (2), 84-114

69. N. Zhou, S. Jiang, T. Huang, M. Qin, T. Hu, J. Luo, Single-phase high-entropy intermetallic compounds (HEICs): Bridging high-entropy alloys and ceramics, Science Bulletin, 2019, Vol. 64, 856-864

70. D. Raabe, C. C. Tasan, H. Springer, M. Bausch, From high-entropy alloys to high-entropy steels, Steel Research Int., 2015, Vol. 86 (10), 1127-1138

71. O. F. Dippo, N. Mesgarzadeh, T. J. Harrington, G. D. Schrader, K. S. Vecchio, Bulk high-entropy nitrides and carbonitrides, Nature Scientific Reports, 2020, Vol. 10, 21288

72. S. Guo, C. T. Liu, Phase stability in high entropy alloys: Formation of solid-sollution phase or amorphous phase, Progress in Natural Science: Materials International, 2011, Vol. 21, 433-446

73. Y. V. Krishna, U. K. Jaiswal, M. R. Rahul, Machine learning approach to predict new multiphase high entropy alloys, Scripta Materialia, 2021, Vol. 197, 113804 (11 pages)

74. L. J. Santodonato, P. K. Liaw, R. R. Unocic, H. Bei, J. R. Morris, Predictive multiphase evolution in Al-containing high-entropy alloys, Nat. Commun., 2018, Vol. 9, 4520 (10 pages)

75. Y. C. Huang, C. S. Tsao, S. K. Wu, C. Lin, C. H. Chen, Nano-precipitates in severely deformed and low-temperature aged CoCrFeMnNi high-entropy alloy studied by synchrotron small-angle X-ray scattering, Intermetallics, 2019, Vol. 105, 146-152

76. K. H. Lee, S. K. Hong, S. I. Hong, Precipitation and decomposition in CoCrFeMnNi high entropy alloy at intermediate temperatures under creep conditions, Materialia, 2019, Vol. 8, 100445 (10 pages)

77. A. Manzoni, H. Daoud, R. Volkl, U. Glatzel, N. Wanderka, Phase separation in equiatomic AlCoCrFeNi high-entropy alloy, Ultramicroscopy, 2013, Vol. 132, 212-215

78. C. M. Rost, E. Sachet, T. Borman, A. Moballegh, E. C. Dickey, D. Hou, J. L. Jones, S. Curtarolo, J. P. Maria, Entropy-stabilized oxides, Nat. Commun., 2015, Vol. 6, 8485 (8 pages)

79. M. Brahlek, M. Gazda, V. Keppens, A. R. Mazza, S. J. McCormack, A. M. Gryn, B. Musico, K. Page, C. M. Rost, S. B. Sinnott, C. Toher, T. Z. Ward, A. Yamamoto, What is in a name: Defining high entropy oxides, APL Mater., 2022, Vol. 10, 110902 (12 pages)

80. B. L. Musico, D. Gilbert, T. Z. Ward, K. Page, E. George, J. Yan, D. Mandrus, V. Keppens, The emergent field of high entropy oxides: Design, prospects, challenges and opportunities for tailoring material properties, APL Mater., 2020, Vol. 8, 040912 (17 pages)

81. S. Akrami, P. Edalati, M. Fuji, K. Edalati, High-entropy ceramics: Review of principles, production and applications, Materials Science & Engineering R, 2021, Vol. 146, 100644 (64 pages)

82. J. Dabrowa, M. Stygar, A. Mikula, A. Knapik, K. Mroczka, W. Tejchman, M. Danielewski, M. Martin, Synthesis and microstructure of the $(Co,Cr,Fe,Mn,Ni)_3O_4$ high entropy oxide characterized by spinel structure, Materials Letters, 2018, Vol. 216, 32-36

83. A. Sarkar, Q. Wang, A. Schiele, M. R. Chellali, S. S. Bhattacharya, D. Wang, T. Brezesinski, H. Hahn, L. Velasco, B. Breitung, High-entropy oxides: Fundamental aspects and electrochemical properties, Adv. Mater., 2019, 1806236 (9 pages)

84. C. M. Rost, Z. Rak, D. W. Brenner, J. P. Maria, Local structure of the $Mg_xNi_xCo_xCu_xZn_xO$ (x=0.2) entropy-stabilized oxide: An EXAFS study, J. Am. Ceram. Soc., 2017, Vol. 100, 2732-2738

85. G. Anand, A. P. Wynn, C. M. Handley, C. L. Freeman, Phase stability and distortion in high-entropy oxides, Acta Mater., 2018, Vol. 146, 119-125

86. S. J. McCormack, A. Navrotsky, Thermodynamics of high entropy oxides, Acta Mater., 2021, Vol. 202, 1-21

87. A. D. Dupuy, X. Wang, J. M. Schoenung, Entropic phase transformation in nanocrystalline high entropy oxides, Mater. Res. Lett., 2019, Vol. 7 (2), 60-67

88. O. Elmutasim, A. G. Hussien, A. Sharan, S. Alkhoori, M. A. Vasiliades, I. M. A. Taha, S. Kim, M. Harfouche, A. H. Emwas, D. H. Anjum, M. Efstathiou, C. T. Yavuz, N. Singh, K. Polychronopoulou, Evolution of oxygen vacancy sites in ceria-based high entopy oxides and their role in N_2 activation, ACS Appl. Mater, Interfaces, 2024, Vol. 16, 23038-23053 (16 pages)

89. L. Pauling, The principles determining the structure of complex ionic crystals, J. Am. Ceram. Soc., 1929, Vol. 51 (4), 1010-1026

90. W. Hong, F. Chen, Q. Shen, Y. H. Han, W. G. Fahrenholtz, L. Zhang, Microstructural evolution and mechanical properties of (Mg,Co,Ni,Cu,Zn)O high-entropy ceramics, J. Am. Ceram. Soc., 2019, Vol. 102, 2228-2237

91. A. D. Dupuy, M. R. Chellali, H. Hahn, J. M. Schoenung, Nucleation and growth behaviour of multicomponent secondary phases in entropy-stabilized oxides, J. Mater. Res., 2023, Vol.38 (1), 198-204

92. D. Berardan, A. K. Meena, S. Franger, C. Herrero, N. Dragoe, Controlled Jahn-Teller distortion in (MgCoNiCuZn)O-based high entropy oxides, Journal of Alloys and Compounds, 2017, Vol. 704, 693-700

93. C. B. Carter, M. G. Norton, Ceramic Materials Science and Engineering, Springer Nature, USA, 2013, Edition 2, XXXIII (766 pages)

94. Y. M. Chiang, D. P. Birnie, W. D. Kingery, Physical Ceramics Principles for Ceramic Science and Engineering, John Wiley & Sons Inc., USA, 1997 (542 pages)

95. K. E. Sickafus, J. M. Wills, N. W. Grimes, Structure of spinel, J. A. Ceram. Soc., 1999, Vol. 82 (12), 3279-3292

96. J. B. Goodenough, A. L. Loeb, Theory of ionic ordering, crystal distortion, and magnetic exchange due to covalent forces in spinels, Physical Review, 1955, Vol. 98 (2) (18 pages)

97. P. E. Vullum, H. L. Lein, M. A. Einarsrud, T. Grande, R. Holmestad, TEM observations of rhombohedral and monoclinic domains in $LaCoO_3$-based ceramics, Philosophical Magazine, 2008, Vol. 88 (8), 1187-1208

98. K. Behnia, Finding merit in dividing neighbors, Science, 2016, Vol. 351, 6269 (2 pages)

99. S. Massidda, M. Posternak, A. Baldereschi, R. Resta, Noncubic behavior of antiferromagnetic transition-metal monoxides with the rocksalt structure, Phys. Rev. Lett., 1999, Vol. 82 (2), 430-433

100. C. N. R. Rao, P. V. Vanitha, A. K. Cheetham, Phase separation in metal oxides, Chem. Eur. J., 2003, Vol. 9 (4), 829-836

101. V. B. Shenoy, D. D. Sarma, C. N. R. Rao, Electronic phase separation in correlated oxides: The phenomenon, its present status and future prospects, Chem. Phys. Chem., 2006, Vol. 7, 2053-2059

102. Y. Horibe, S. Takeyama, S. Mori, Large-scale phase separation with nano-twin domains in manganite spinel $(Co,Fe,Mn)_3O_4$, AIP Conference Proceedings, 2016, 1763, 050005 (6 pages)

103. A. S. Pal, A. K. L. Das, K. Gururaj, M. Sadhasivam, K. M. Knowles, Md. I. Ahmad, K. G. Pradeep, J. Basu, Nanoarchitectonics of self-assembled chessboard-like

structures by recurrent phase separation and coalescence of nano domains in CoFeMn oxide, Acta Mater., 2023, 242, 118423 (12 pages)

104. A. S. Pal, A. K. L. Das, A. Singh, K. M. Knowles, Md. I. Ahmad, J. Basu, Evolution of a self-assembled chessboard nanostructure spinel in a CoFeGaMnZn multicomponent oxide, Philosophical Magazine, 2022, Vol. 102 (12), 1121-1135

105. A. Singh, S. Yasui, A.S. Pal, L.A. Bendersky, I. Takeuchi, R.K. Mandal, J. Basu, Structure and interfaces of compositionally graded $Li(Ni,Mn)_xO_y$ cathodes on (111) Nb-doped $SrTiO_3$, Philosophical Magazine, 2022, 102, 1547-1579

106. B. G. Hyde, A. N. Bagshaw, Some defect structures in crystalline solids, Annu. Rev. Mater. Sci., 1974, Vol. 4, 43-92

107. J. S. Anderson and R. J. D. Tilley, Crystallographic shear in oxygen-deficient rutile: An electron microscopic study, Journal of Solid State Chemistry, 1970, Vol. 2 472-482

108. R. J. D. Tilley, The formation of shear structures in sub-stoichiometric tungsten trioxide, Mat. Res. Bull., 1970, Vol. 5, 813-824

109. R. J. D. Tilley, An electron microscope study of perovskite-related oxides in Sr-Ti-O system, Journal of Solid State Chemistry, 1977, Vol. 21, 293-301

110. A. Schron, C. Rodl, F. Bechstedt, Crystalline and magnetic anisotropy of the 3d-transition metal monoxides MnO, FeO, CoO and NiO, Physical Review B, 2012, Vol. 86, 115134

111. P. K. Davies, M. Akaogi, Phase intergrowths in spinelloids, Nature, 1983, Vol. 305, 788-790

112. C. Oses, C. Toher, S. Curtarolo, High-entropy ceramics, Nat. Rev. Mater., 2020, Vol. 5, 295-309

113. M. Anandkumar, E. Trofimov, Synthesis, properties, and applications of high-entropy oxide ceramics: Current progress and future perspectives, Journal of Alloys and Compounds, 2023, Vol. 960, 170690

114. A. C. Yeh, S. Gorsse, V. Keppens, D. A. Gilbert, Design and development of high entropy materials, APL Materials, 2023, Vol. 11, 030402

115. J. B. Goodenough, Perspective on engineering transition-metal oxides, Chemistry of Materials, 2014, Vol. 26, 820-829

116. D. Berardan, S. Franger, D. Dragoe, A. K. Meena, N. Dragoe, Colossal dielectric constant in high entropy oxides, Phys. Status Solidi RRL, 2016, Vol. 10 (4), 328-333

117. D. Berardan, S. Franger, A. K. Meena, N. Dragoe, Room temperature lithium superionic conductivity in high entropy oxides, J. Mater. Chem. A, 2016, Vol. 4, 9536-9541

118. Z. Y. Liu, Y. Liu, Y. Xu, H. Zhang, Z. Shao, Z. Wang, H. Chen, Novel high-entropy oxides for energy storage and conversion: From fundamentals to practical applications, Green Energy and Environment, 2023, Vol. 8, 1341-1357

119. Z. Lun, B. Ouyang, D. H. Kwon, Y. Ha, E. E. Foley, T. Y. Huang, Z. Cai, H. Kim, M. Balasubramanian, Y. Sun, J. Huang, Y. Tian, H. Kim, B. D. McCloskey, W. Yang, R. J. Clement, H. Ji, G. Ceder, Cation-disordered rocksalt-type high entropy cathodes for Li-ion batteries, Nature Materials, 2021, Vol. 20, 214-221

120. Q. Wang, A. Sarkar, Z. Li, Y. Lu, L. Velasco, S. S. Bhattacharya, T. Brezesinski, H. Hahn, B. Breitung, High entropy oxides as anode material for Li-ion battery applications: A practical approach, Electrochemistry Communications, 2019, Vol. 100, 121-125

121. S. H. Albedwawi, A. Aljaberi, G. N. Haidemenopoulos, K. Polychronopoulou, High entropy oxides-exploring paradigm of promising catalysts: A review, Materials and Design, 2021, Vol. 202, 109534 (27 pages)

122. S. Zhai, J. Rojas, N. Ahlborg, K. Lim, M. F. Toney, H. Jin, W. C. Chueh, A. Majumdar, The use of poly-cation oxides to lower the temperature of two-step thermochemical water splitting, Energy Environ. Sci., 2018, Vol. 11, 2172-2178

123. J. Baek, M. D. Hossain, P. Mukherjee, J. Lee, K. T. Winther, J. Leem, Y. Jiang, W. C. Chueh, M. Bajdich, X. Zheng, Synergistic effects of mixing and strain in high entropy spinel oxides for oxygen evolution reaction, Nat. Commun., 2023, Vol. 14 (5936), 1-11

124. J. Zhang, R. P. Hermann, Long-range antiferromagnetic order in a rocksalt high entropy oxide, Chem. Mater., 2019, Vol. 31, 3705-3711

125. M. P. J. Segura, T. Takayama, D. Berardan, A. Hoser, M. Reehuis, H. Takagi, N. Dragoe, Long-range magnetic ordering in a rocksalt-type high-entropy oxides, Appl. Phys. Lett., 2019, Vol. 114, 122401 (6 pages)

126. J. L. Braun, C. M. Rost, M. Lim, A. Giri, D. H. Olson, G. N. Kotsonis, G. Stan, D. W. Brenner, J. P. Maria, P. E. Hopkins, Charge-induced disorder controls the thermal conductivity of entropy-stabilized oxides, Adv. Mater., 2018, Vol. 30, 1805004 (8 pages)